DEVELOPMENT OF STEREOCOMPLEX POLYLACTIC ACID AEROGEL FOR REMOVING POLYETHYLENE TEREPHTHALATE MICROPLASTICS IN WATER

A Thesis

Presented to

The Faculty of the Department of Chemistry and Biochemistry

California State University, Los Angeles

In Partial Fulfillment

of the Requirements for the Degree

Master of Science

in

Chemistry

By

Dang Khoa Phuoc Tran

May 2025

© 2025

Dang Khoa Phuoc Tran

ALL RIGHTS RESERVED

The thesis OR project report of Dang Khoa Phuoc Tran is approved.

Dr. Petr Vozka, Committee Chair

Dr. Brenda Andrade Rounds

Dr. Linda Tunstad

Dr. Yangyang Liu

Dr Krishna Foster, Department Chair

California State University, Los Angeles

May, 2025

TABLE OF CONTENTS

Abstract v

Acknowledgments vi

List of Tables vii

List of Figures viii

Chapter

1. Background 1

2. Materials and Methods 5

2.1 Materials 5

2.2 Manufacturing of sc-PLA Arogel 5

2.3 Characterization 7

2.3.1 X-Ray Diffractometry 7

2.3.2 Scanning Electron Microscopy 7

2.3.3 Measurement of porosity via Adsorption Isotherm 8

2.4 Adsorption Experiment 8

3. Results and Discussion 10

3.1 Porous sc-PLA Aerogel as freeze-dried polymer product 10

3.2 Characterization of sc-PLA aerogel 11

3.2.1 Stereocomplexity via XRD 11

3.2.2 Porous morphology of sc-PLA aerogel via SEM 13

3.2.3 Characterization of nanopores of sc-PLA aerogel via adsorption isotherm 15

3.3 Adsorption of PET microplastics in water 18

4. Conclusion 25

References.....26

ABSTRACT

Stereocomplex-Polylactic Acid Aerogels for Removal of Polyethylene Terephthalate Microplastics in Water via Adsorption

By Dang Khoa Phuoc Tran

Microplastics (MPs) are degraded fragments of large-sized plastics with dimensions of $\leq$ 5 mm. Their release into the environment, mainlyin water, carries potentially harmful effects on humans and marine ecosystems. As a result, several studies have focused on developing sustainable aerogels that can effectively adsorb and remove microplastics (MPs) from water. In this project, we manufacture porous aerogels from stereocomplex polylactic acid (sc-PLA), a biodegradable biopolymer. The adsorbents are created by mixing an equimolar ratio of two enantiomeric forms of PLA, poly-D-lactide and poly-L-lactide, in 1,4-dioxane and then freeze-drying.. For characterization, X-ray diffractometry (XRD) and scanning electron microscopy (SEM) confirm the aerogel's stereocomplex crystallinity and porous structure, respectively. Adsorption isotherm of nitrogen gas detects the presence of nano scale pores and provides additional porosity parameters. The adsorption capacity of polyethylene terephthalate microplastics on sc-PLA aerogels is determined after 18 hours. Data analysis utilizes the adsorption kinetic models (i.e., pseudo-first-order kinetic, pseudo-second-order kinetic, and intra-particle diffusion) to explain the multiphase adsorption mechanism.

ACKNOWLEDGEMENT

I would like to express my gratitude to my committee members, Dr. Petr Vozka, Dr. Brenda Andrade Rounds, Dr. Yangyang Liu, and Dr. Linda Tunstad, for their valuable input during the conception of my thesis. I am especially grateful to Dr. Brenda Andrade Rounds for granting me access to her lyophilizer, to Dr. Yangyang Liu and fellow graduate students of the Yangyang Liu Research Group for assisting me with the technique of adsorption isotherm and XRD, and to Dr. Mohsen Eshraghi and Patrick Hartunian for providing me with service at the Materials Characterization Laboratory. I also would like to extend my gratitude to the CATSUS Fellowship for providing me with the resources and support for the completion of my thesis (NSF award HRD-2112554).

Above all, I am deeply grateful to Dr. Vozka for his invaluable support and mentorship during my academic career at Cal State LA.

LIST OF TABLES

Table

1. Parameters of micropores and mesopores detectable from the adsorption isotherm (with N_2 gas at 77 K) of sc-PLA aeroge 17

2. Parameters of intraparticle diffusion model for sc-PLA aerogel, representing three phases: external film diffusion (1), interparticle diffusion (2), and saturation (3).....23

LIST OF FIGURES

Figure

1. Stereochemical mechanisms of stereocomplex PLA 3

2. Manufacturing scheme of sc-PLA aerogel of equimolar ratio of PDLA and PLLA in a sequence of isothermal annealing at 60 °C, thermal-induced phase separation (gelation) at -12 °C for 24 hrs, and lyophilization up to 72 hrs 6

3. Measurements of sc-PLA aerogel final product after freeze-drying for (a) depth and (b) diameter 10

4. Literature XRD patterns of PLLA and sc-PLA aerogels with different content of PDLA for oil-water separation.....11

5. Experimental XRD pattern of sc-PLA aerogel at equimolar ration (1:1) of PDLA and PLLA.....12

6. Experimental SEM images at (a) ~300x and (b) ~1000x magnification of porous sc-PLA aerogel 13

7. Experimental pore size distribution of sc-PLA aerogel for removing PET MPs in water via ImageJ analysis of SEM image 14

8. Literature SEM images and pore size distribution of equimolar sc-PLA aerogel for oil-water separation.....15

9. Pore size distribution of sc-PLA aerogel via adsorption isotherm with N_2 gas at constant 77 K 16

10. The adsorption capacity of experimental PET MPs in water being adsorbed by sc-PLA aerogel 19

11. Adsorption (a) pseudo-first-order and (b) pseudo-second-order kinetic models of absorbed PET MPs in water onto sc-PLA aerogel at room temperature 20
12. Intraparticle diffusion models in three adsorption phases, external film diffusion (a), interparticle diffusion (b), and saturation (c), of PET MPs adsorbed by sc-PLA aerogel at 25°C 22

CHAPTER 1

BACKGROUND

Microplastics (MPs), defined as plastic particles or fragments of dimension equal to or less than 5 millimeters [1], have garnered tremendous interest from researchers. Being abundant in the environment, especially water, they potentially harm marine species and humans [2,3]. Their degradability in nature is also limited and only smaller, finer MPs arefurtherly fragmented . Therefore, removing MPs from water is imperative in maintaining the wellness of the marine ecosystem and human life. Waste water treatment plants (WWTPs) using filtration techniques, such as disc filters and rapid sand filtration [3], only remove up to 90% of MPs [2]. One of the most common type of MPs in water is polyethlene terephthalate (PET) from fragments of polyester fiber [2]. They contribute ~35% of the total global MPs pollution due to their popularity in commodity plastics and difficulty of being removed by WWTPs. Concerning the rest of the unfiltered MPs entering and accumulating in the environment, researchers have focused on adsorption as an effective and facile method of removal [1,2]. With a common objective of sustainable development, studies have observed the adsorption effectiveness of many bio-based materials, including biochar, polysaccharide sponges, and foams [3].

Amongst other developments in adsorption techniques, many have proposed aerogels as porous and light-weight adsorbents that offer significant economic value and removal efficiency [1,2]. In water remediations, the application of aerogels has been found in oil-water separation [4,5], toxicant removal [6], and MP removal [1,2,3], which offers more research opportunities. Physisorption and chemisorption are mainly responsible for the adsorption mechanism of MPs onto aerogels [1,2]. Possessing highly porous morphology,

aerogels entrap tiny plastic particles within their structure [2]. Consequently, studies have selected polysaccharides, such as chitosan and cellulose, and other celluloses as materials for aerogels [1,2]. Their high porosity optimizes adsorption via both physical and chemical interaction. However, susceptible to hydrolysis, polysaccharide-based aerogels are unstable in water and thus have limited reusability [7]. More opportunities are opening up for alternative materials, specifically biopolymers, that can improve the hydro stability of aerogels.

Polylactic acid (PLA) is one of the most common biopolymers that offers good mechanical properties, hydrophobicity, tunability, and biodegradability [4,8,9]. Its bio-based origin, derived from renewable materials such as corn, sugar, and starch, degrades into water and carbon that pose little to no toxicity to the environment [6,9,10]. In water remediation, PLA has been developed into aerogels, foams, fibrils, and other porous materials in oil-water separation and pollutant removal [11,12]. Yet MPs' removal remains an opportunity for the application of PLA aerogels. As a hydrophobic bio-based polymer, PLA has become an appropriate material for making porous adsorbents. Studies have focused on improving porosity, hydrophobicity, and durability to optimize adsorption and recyclability. PLA-based aerogels possess good porosity, though it varies depending on the method of drying (i.e., freeze drying, supercritical CO_2 drying) [6]. The inherent hydrophobicity of PLA proves that it can be stable in water. According to the experiment of Benito-González et al., it can be used as a hydrophobic coating for cellulose-based aerogels [7]. Yet even in solid form, PLA is a brittle plastic. Researchers have explored the benefits of its stereocomplex (SC) form, addressing the limits of mechanical and thermal durability of PLA. Stereocomplex-PLA (sc-PLA) is the result of mixing two enantiomeric

forms, poly-L-lactide (PLLA) and poly-D-lactide (PDLA). The equimolar ratio of PLLA: PDLA, equal to 1:1, produces samples with the most SC crystallites, without homo-crystallites [4]. Not only possessing superior mechanical and thermal properties compared to neat PLA [5,10,13], sc-PLA porous materials also show improved porosity [4] and hydrophobicity [4,8]. These enhancements are possible due to the packing of the stereocomplex helices, which are stabilized by strong van der Waals interactions and hydrogen bonding between the methyl hydrogen of one PLA compound and the carbonyl oxygen of its respective enantiomeric PLA compound [14].

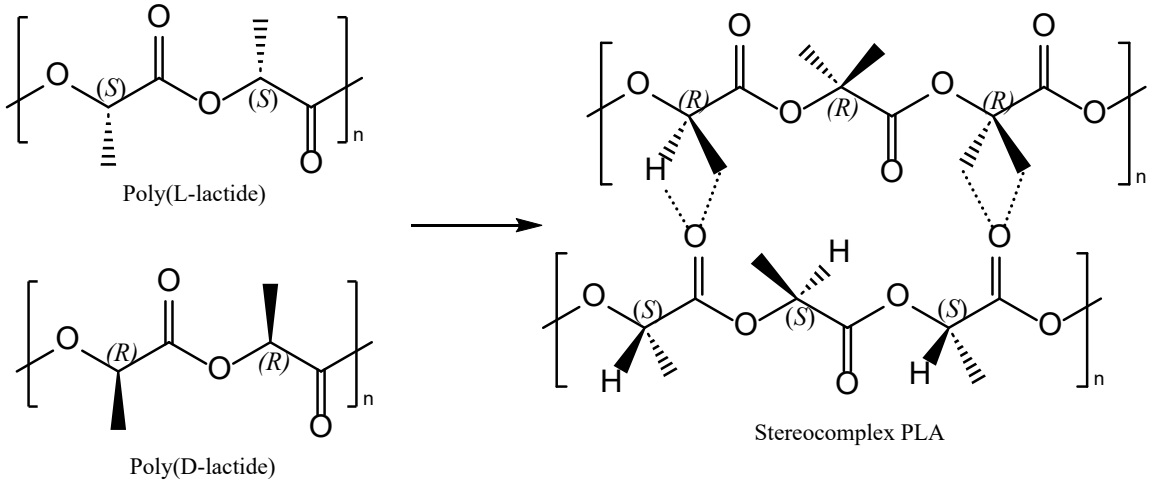


Figure 1. Stereochemical mechanisms of stereocomplex PLA

With a grave concern of the harmful impacts of MPs in water, a sustainable aerogel was manufactured via freeze-drying using an equimolar mixture of two PLA enantiomers, PDLA and PLLA, the content of which enhanced the formation of SC crystals within the polymer matrix. The final product was a lightweight, hydrophobic, and porous adsorbent intended to remove PET microplastics in water. Especially concerning the MPs, the network of micron sized poresthroughout the structure of aerogel was able to capture the adsorbate via physisorption. This comprehensive study is the first to propose the use of sc-

PLA aerogel as an effectivematerial for removing PET MPs in water. This project is divided into three parts, (1) the manufacturing method of sc-PLA aerogel via lyophilization, (2) the characterization of the aerogel product using XRD, SEM, and adsorption isotherm with N_2 gas, and (3) the adsorption experiment on PET MPs.

CHAPTER 2

Materials and Methods

2.1 Materials

Solid polylactic acid in two enantiomeric forms, poly(D)lactide (PDLA, Mn 25,000-35,000 Da) and poly(L, D 96:4- lactide, Mn 80,000-120,000 Da) acid, are obtained from Amerigo Scientific, New York, USA. For the mixing agent, 1,4-dioxane obtained from Fischer Scientific™, New Jersey, USA, was selected because of its similarpolarity to the PLA ingredients. Ultrafine polyethylene terephthalate powder (>99% purity), obtained from Nanochemazone™, Edmonton, Canada, of two size populations of 2 – 15 μm and 58 – 120 μm, was used for the adsorption experiments as targeted MPs in water. Other chemicals included acetone and commercial dry ice for freeze-drying via a benchtop lyophilizer.

2.2 Manufacturing of sc-PLA aerogel

The manufacturing of sc-PLA aerogel followed the procedures proposed by Chen et al. [4] and Yin et al.[15] available techniques. A comprehensive manufacturing scheme is presented in Figure 2.



Figure 2. Manufacturing scheme of sc-PLA aerogel of equimolar ratio of PDLA and PLLA in a sequence of isothermal annealing at 60 °C, thermal-induced phase separation (gelation) at -12 °C for 24 hrs, and lyophilization up to 72 hrs

A total of 0.250 g of PLLA and PDLA of equimolar (1:1), was mixed in a solution consisting of 8.3 mL of 1,4-dioxane as the organic solvent and 0.33 mL of deionized water. PLA's 3% mass concentration was found to be critically minimal for manufacturing PLA-based aerogels [15,16]. To achieve a homogenous solution in which the PLA crystals would be evenly dispersed, the mix of 1,4-dioxane and deionized water as the organic solvent facilitated the self-polymerization of the two enantiomers and promoted the formation of SC crystals. The solvent selection was appropriate for the method of freeze-drying (i.e., lyophilization). The solution was heated at 60 ºC and stirred using a magnetic stirrer until completely dissolved and homogenous. Applying heat during the isothermal annealing of the PLA solution promoted the formation of sc-crystals by reorganizing disordered homo-crystals [8]. Then, the well-mixed solution was allowed to cool for 30 minutes before being transferred into a freezer at -12ºC for 24 hours.This process, called the thermal induced phase separation (or gelation) allows the polymer to separate from the solvent and form solid, porous structure [14]. The frozen gel was transferred into a freeze-drying flask attached to one of the ports of a LABCONCO® Dry-ice Benchtop Freeze Dryer Lyophilizer, available at Dr. Brenda Andrade Rounds Laboratory at Cal State LA. A dry-

ice bath in acetone was prepared inside the cooling chamber of the lyophilizer to capture the sublimed solvent. Due to the lyophilizer's setup, frozen samples were susceptible to melting at atmospheric temperature (i.e., 25 ºC) and were at risk of structural collapse. As the solution, the drying flask was dipped into an ice bath to prevent the samples from melting. Samples were freeze-dried under a vacuum at 3000 microns Hg for up to 72 hours. These conditions (i.e., frozen samples under high pressure) allowed the slow sublimation of the solvent, thus creating the porous structure of sc-PLA aerogel.

2.3 Characterization

2.3.1 X-Ray Diffractometry

The crystalline structure of sc-PLA aerogel was determined using an X-ray diffractometer (Bruker D2 PHASER Gen 2 Benchtop XRD, Karlsruhe, Germany) available at the Materials Characterization Laboratory at Cal State LA. X-ray diffraction (XRD) works by shining X-rays on a material, primarily crystalline solids, and analyzing the scattered X-rays. The diffraction pattern is determined from the analysis of the constructive and destructive interference of the scattered X-rays [17]. The diffractometer was set at 30V and installed with a 0.2-mm divergence slit. The detection range of 2θ was set from 5 to 30 degrees for detection of the SC crystal planes. Confirming the presence of SC crystals is critical in explaining its impacts on the aerogel's porosity and consequently adsorption effectiveness.

2.3.2 SEM Morphology Imaging

The visual inspection of a section of the aerogel provided a representative depiction of its porous structure. The morphology of sc-PLA aerogel was imaged by scanning electron microscopy (Quanta FEI 200 SEM), which is available at the Materials Characterization Laboratory at Cal State LA. The basic principle of SEM involves using a

focused beam of electrons that excites the sample. The detector captures the various signals emitted by the excited atoms and provides high-definition images of the structure and topography [18]. The microscope was placed in high vacuum mode at a pressure of 6.4 x 10^{-5} mbar and a high voltage of 15 kV. Both magnifications were enhanced at spot size 5.0 and high definition 2048x1768. No metallic coating was applied to the surface of the aerogel.

2.3.3 Measurement of porosity via Adsorption Isotherm

Due to the non-uniform and micro-sized porous structure of biopolymer-based aerogel, the quantification of porosity (i.e., pore size and distribution) was analyzed via adsorption isotherm. The analysis was provided by Dr. Yangyang Liu's Research Group at Cal State LA using Micromeritics® High-Performance Gas Adsorption Analyzer ASAP 2020. A sample of 35.4 mg of sc-PLA aerogel was prepared for analysis, with the condition set at a cryogenic temperature of 77 K, and the adsorbate gas was nitrogen. The isotherm was set under a pressure of 100 mmHg.

2.4 Adsorption Experiment

The adsorption experiment determines the adsorption capacity of sc-PLA aerogel in removing micron-sized PET in water and its adsorption mechanism. The research of Zheng et al. offered a comprehensive and replicable procedure of adsorption experiments of cellulose-basedaerogels to remove MPs in water [2]. Our investigation applied the extensive procedure to achieve three main objectives, namely, (1) to quantify the adsorption capacity, (2) to integrate the adsorption kinetic, and (3) to determine the adsorption mechanism of sc-PLA aerogel.

Ten samples of micron-sized PET solution in water at 300 mg/L concentration were prepared in separated Erlenmeyer flasks. An equal amount of stereocomplex-PLA aerogel was added into each flask and placed on a Lab-line 3520 orbit shaker set at 50 rpm at room temperature. Following the adsorption, the aerogel was removed, and the remaining MPs in solution were filtered and weighedweighed at 10 different time intervals: 0.5, 1, 1.5, 2, 2.5, 3.5, 5, 8, 10, and 18h. A paper filter of 2.5 μm in pore size in consideration to the particle size of PET MPs. The weighing was done using an analytical balance with readability of 0.1 mg.The results provided inputs for the following equation of adsorption capacity [2]:

$$Q = \frac{m_0 - m_t}{W}, \quad (1)$$

where Q is the amount of adsorbed MPs per unit of weight aerogel (mg g^{-1}), m_0 (g) is the initial weight of MPs, and m_t (g) represents the weight of unadsorbed MPs at t time. W (g) is the weight of the added aerogel. The result collected after 18 hours quantified the overall adsorption capacity of aerogel, while the rest of the data at different time intervals were used to integrate the adsorption kinetics and mechanism

CHAPTER 3

Results and Discussion

3.1 Porous sc-PLA aerogel as freeze-dried polymer product

After freeze-drying, sc-PLA aerogel was removed from the vial container, which had molded its shape. The final product was an opaquely white, intact, non-sticky, and flaky plug with a rough surface. The initial visual inspection of aerogel was vital in determining the completion of the freeze-drying process. Figure 3 presents the measurements and displays a visual presentation of the aerogel.

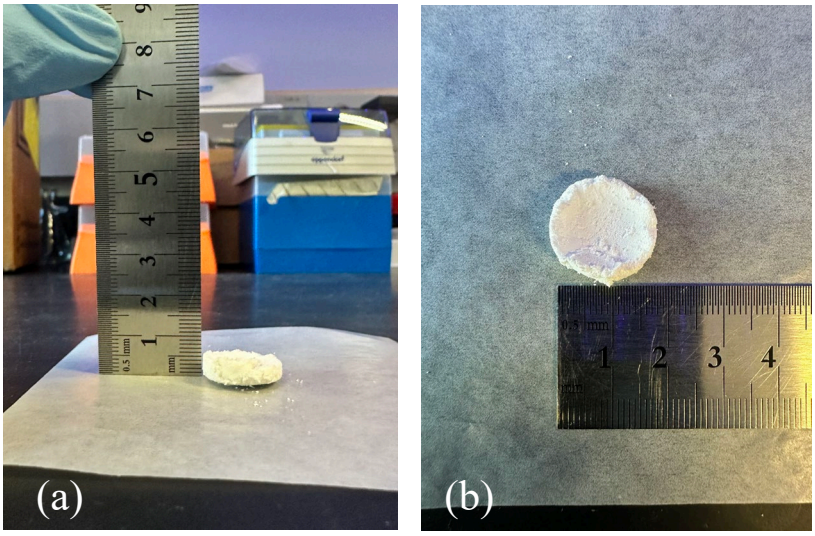


Figure 3. Measurements of sc-PLA aerogel final product after freeze-drying for (a) thickness (0.6 mm) and (b) diameter (1.75 mm)

The aerogel's intact structure, resulted from the self-polymerization of PLLA and PDLA in 1,4-dioxane as the solvent. The high concentration of PDLA, the crystalline enantiomer of PLA, provided a greater degree of crystallinity and durability for the structure of the aerogel during the freeze-drying process.

3.2 Characterization of sc-PLA aerogel

3.2.1 Stereocomplexity via XRD

Every polymer product typically contains both amorphous and crystalline regions. The formation of stereocomplex crystals is a prominent feature that enhances the overall crystallinity of the aerogel structure and its mechanical properties. Especially concerning the significance of such stereocomplexity in enhancing porosity, it is imperative to confirm the prominent presence of SC crystals via X-ray diffractometry. Chen et al. [4] investigated the degree of stereocomplexity of several PLA aerogels with increasing contents of PDLA. Their XRD patterns are presented in Figure 4. Being the crystalline enantiomer of PLA, PDLA significantly contributes to the overall crystallinity of the samples [4]. At an equimolar composition, where PDLA constitutes 50 wt% of the solid content, the XRD pattern displays the greatest crystallinity of SC crystallites, constituting < 40% [4].

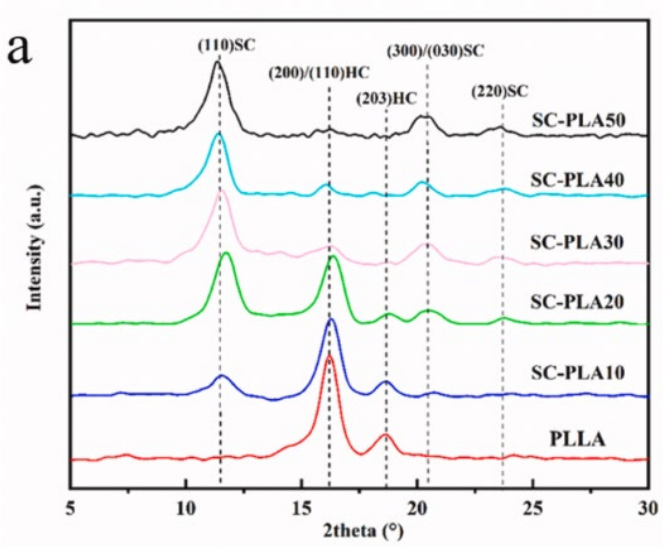


Figure 4. Literature XRD patterns of PLLA and sc-PLA aerogels with different content of PDLA for oil-water separation [4]

In literature, the higher concentration of PDLA in the SC mix results in greater SC crystallinity [4,8,10]. Figure 5 confirms the presence of sc-crystallites with three prominent peaks at 2θ of 11.8º, 20.6º, and 23.8º. They are attributed to the (110), (300)/(030), and (220) crystal planes of SC and are consistent with the XRD patterns of other sc-PLA aerogels reported in literature [4,8,10]. A soft peak at 2θ of 16.7 º (200/110) [8] appears on the experimental and literature XRD patterns [4] of equimolar sc-PLA aerogels indicating a small presence of homo crystals. The neat content of any one of the PLA enantiomers only results in the formation of homo crystals [4,8] for the formation of stereocomplexity requires both enantiomeric compounds. Yet, the prominent presence of SC crystals suggests their promising impacts on the porosity and adsorption effectiveness of this study's sc-PLA aerogel. It is indeed mentionable the preliminary importance of material selection (of PDLA/PLLA content) in designing the appropriate crystallinity.

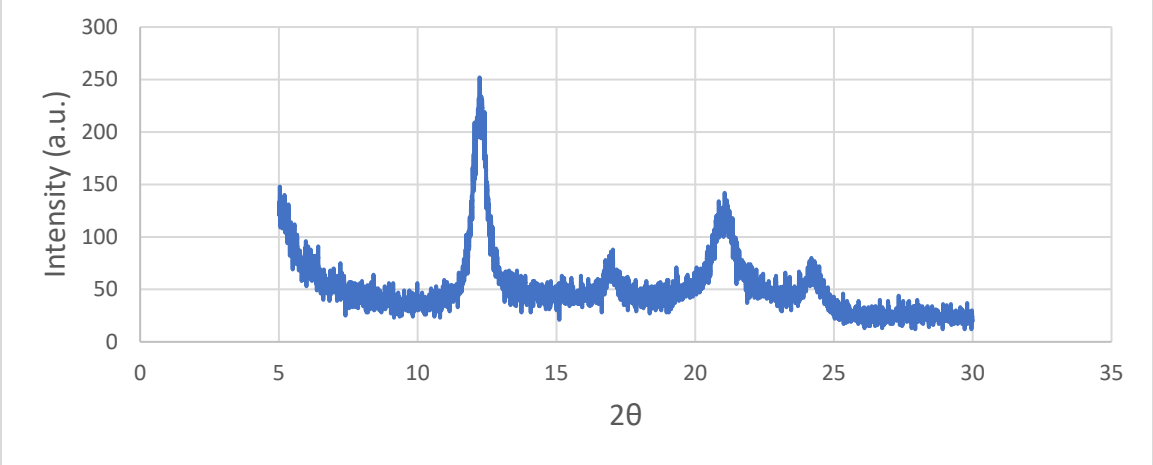


Figure 4. Experimental XRD pattern of sc-PLA aerogel at equimolar ration (1:1) of PDLA and PLLA

3.2.2 Porous morphology of sc-PLA aerogel via SEM

SEM further investigated the porous structure of sc-PLA aerogel. The imaging result is shown in Figure 6(a)(b) depicting the topography of a representative region. The specific parameters of the Quanta FEI SEM offered an optimized inspection of the morphology while retaining the integrity of its porosity. This was possible due to the omission of metallic coating (i.e., gold) which could alter the sample's surface [19]. At ~300x magnification, Figure 6(a) displays a coral-like structure of uneven roughness. Macropores (>50 nm) [20] at micron-scale are visibly present.

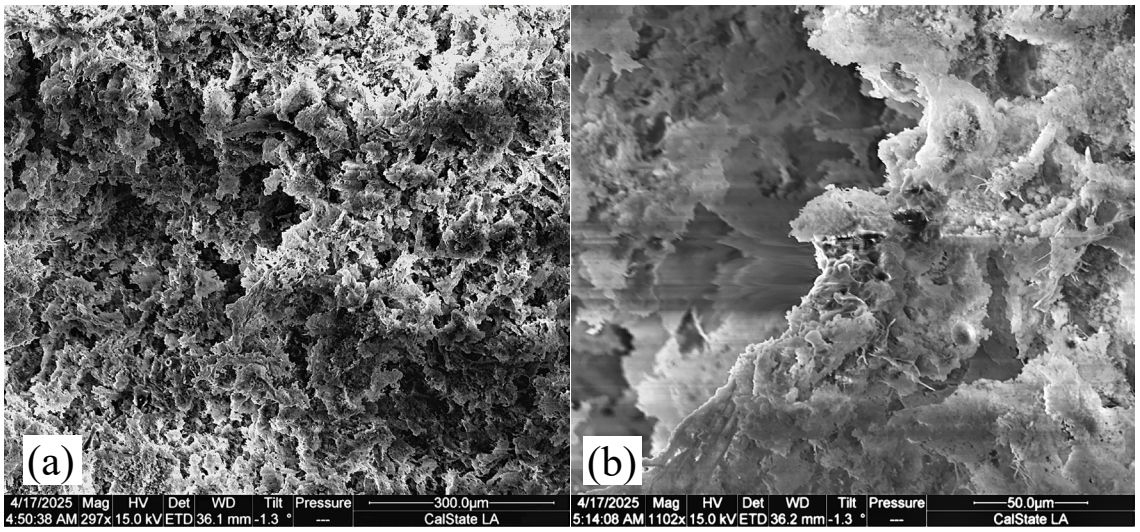


Figure 6. Experimental SEM images at (a) ~300x and (b) ~1000x magnification of porous sc-PLA aerogel

To quantify the exact pore size range, we processed the SEM results using the ImageJ software. The average pore size is 101.06 µm and the pore size distribution is presented in Figure 7.

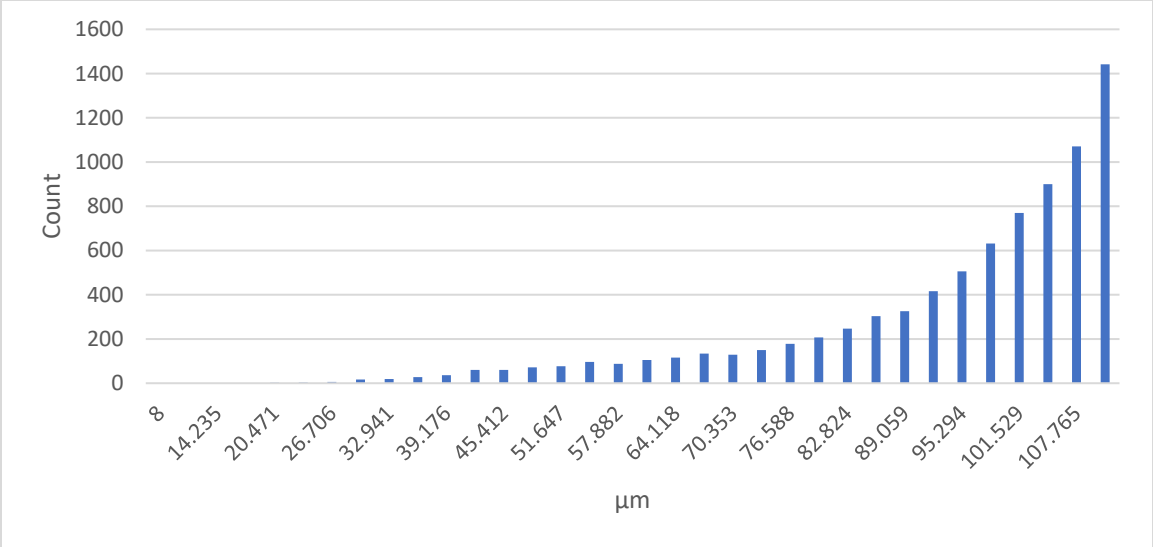


Figure 7. Experimental pore size distribution of sc-PLA aerogel for removing PET MPs in water via ImageJ analysis of SEM image

The experimental average pore size is considerably larger than the literature result (28.11 µm) [4] of the sc-PLA aerogel sample reported in Chen et al. of similar PDLA/PLLA content and method of manufacturing. For reference, the literature's SEM images and pore size distribution of the equimolar sc-PLA aerogel are presented in Figure 8. The porosity discrepancy between the experimental and the literature could be explained by the differences of PLA content (i.e., molecular weight, PDLA:PLLA ratio) and the manufacturing parameters [6], possibly the freeze-drying process (i.e., direct freeze-drying under vacuum in the literature [4] vs. lyophilization in the experiment). Our gelation process was also set at a higher temperature (-12 °C) than theirs (-40 °C) [4]. In general, the porosity of PLA aerogel is determined by various factors including the molecular weight of the polymer, polymer concentration, cooling temperature, freeze-drying methods, solvent selection, and other manufacturing parameters [6]. Therefore, it is reasonable that the experimental porosity is unique compared to the literature.

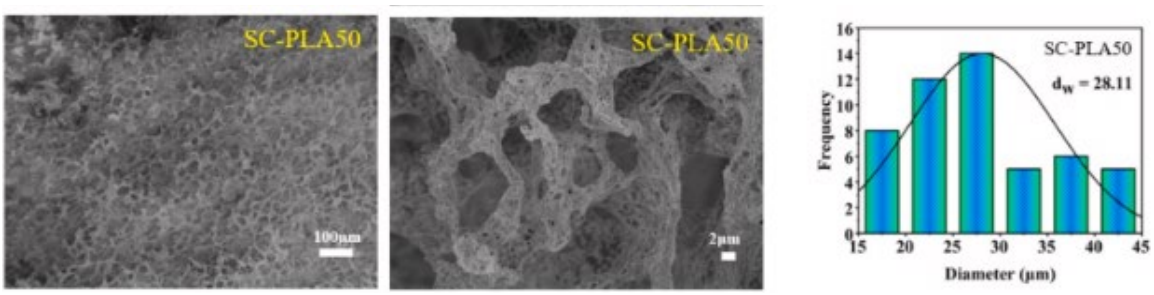


Figure 8. Literature SEM images and pore size distribution of equimolar sc-PLA aerogel for oil-water separation [4]

Greater magnification of ~1000x in Figure 6(b) reveals short-fibril pore texture. This highly porous topography was constructed during the freeze-drying process. Frozen crystals of 1,4-dioxane and deionized water slowly sublimed into gaseous particles, escaping the polymeric matrix and creating an accessible network of interconnected pores diffusing deeply throughout the aerogel. Such porosity structure, typically defined as open pores for their accessibility to gas, fluids, and suspensions [21,22], is suitable for the adsorption of PET MPs in water.

3.2.3 Characterization of nanopores of sc-PLA via Adsorption Isotherm

Interestingly, the reference study of Chen et al. observed the presence of nanopores (1-100 nm) [20] within the structure of their sc-PLA aerogel sample [4]. Upon closer inspection of Figure 6(b), ultrafine pores are clearly visible on the wall of larger pore walls, which optimized the surface area of the adsorbent. Their detection indicates possible presence of mesopores (2-50 nm) and micropores (<2 nm) [20]. As expected, the pore size distribution presented in Figure 9 from the adsorption isotherm with nitrogen gas confirm their presence within the porosity matrix.

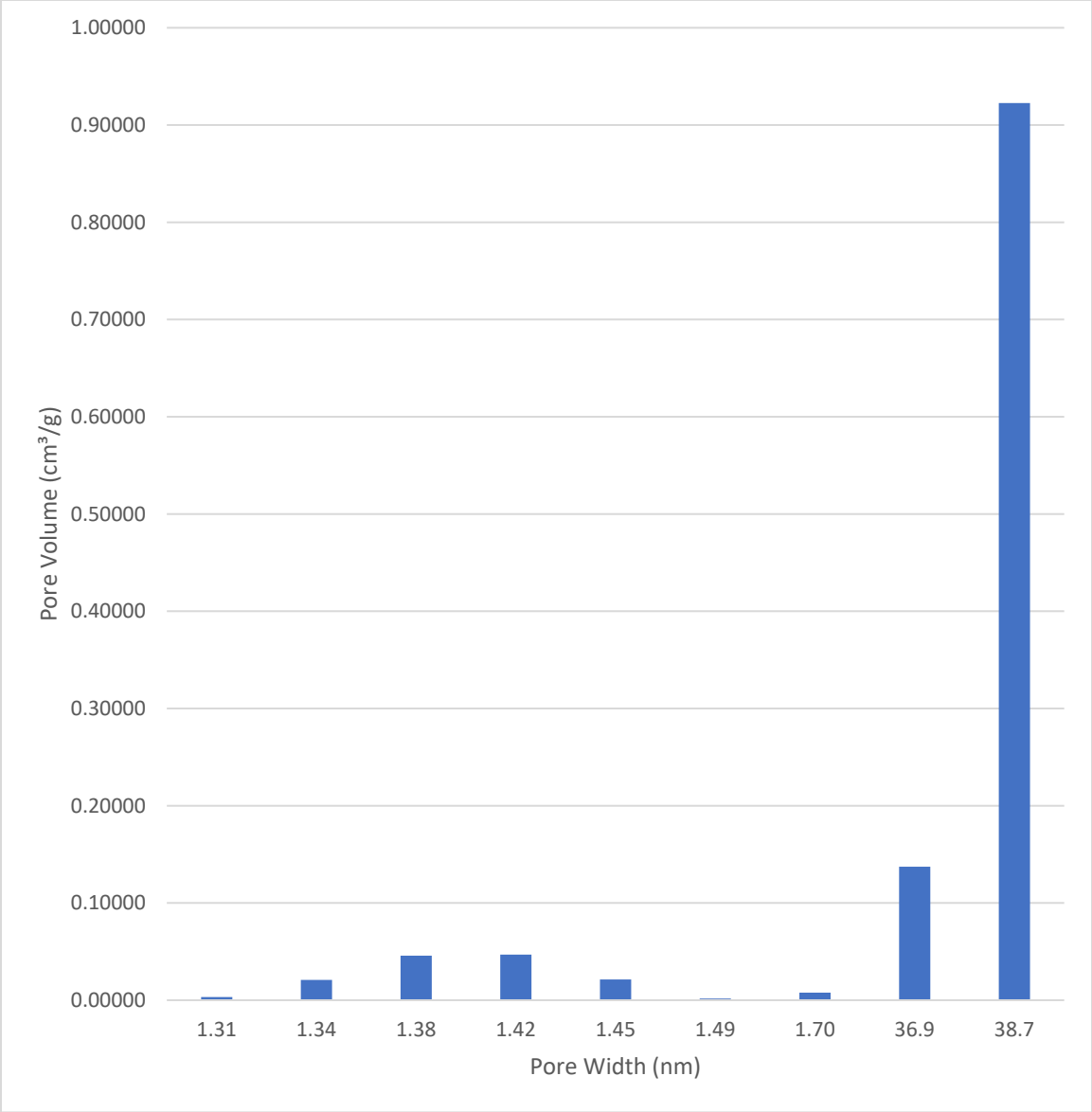


Figure 9. Pore size distribution of sc-PLA aerogel via adsorption isotherm with N_2 gas at constant 77 K

The adsorption isotherm data show a narrow range of detectable micropores and mesopores. They are divided into two sub sets according to their appropriate pore size category and tabulated in Table 1.

Table 1. Parameters of micropores and mesopores detectable from the adsorption isotherm (with N_2 gas at 77 K) of sc-PLA aerogel

Pore size category	**Pore width (nm)**	**Pore size category width median (nm)**	**Pore volume (cm^3/g)**	**Pore size category pore volume median (cm^3/g)**
Micropore (<2 nm)	1.31	1.42	0.00334	0.0210
	1.34		0.0209	
	1.38		0.0458	
	1.42		0.0470	
	1.45		0.0213	
	1.49		0.00175	
	1.70		0.00786	
Mesopore (2-50 nm)	36.9	37.8	0.137	0.530
	38.7		0.923	

The detection of nanopores (1-100 nm) [6,20] widens the overall pore size range of the aerogel. Noticably, the accumulate volume of mesopores is greater than that of micropores suggesting its dominant presence within the nanopore size range. This is consistent with the finding reported in Milanovic et al. [6] in which mesopores (of median ~3.55 nm) are present in all PLA aerogel samples. Their average pore volume (~1.0583 cm^3/g) [6] is a reference to the pore abundance. Particularly, the volume (0.923 cm^3/g) of the experimental 38.7-nm mesopores is comparable to the literature value.

In addition to the visible open porosity, the preliminary inspection of the SEM images reveals a multi-scale hierarchical pore network ranging from micropores to macropores. This structure is favorable for mass transfer and enhances the material's potential for adsorption-based applications. Most importantly, the micron-size range and the highly porous structure are appropriate parameters for the adsorption and capturing of the micron-sized PET sample of which pore size ranges from 2-120 μm. The short-fibril features observed on the pore walls likely result from the crystallization of stereocomplex PLA chains, contributing to the stability and surface area of the structure. Notably, no signs

of pore collapse or densification were observed, indicating that the stereocomplexation also helped maintain mechanical integrity during freeze-drying.

3.3 Adsorption of PET microplastics in water

The adsorbed amounts of PET at ten different time intervals were deduced from weighing the PET left inside the solution from which the treated aerogel was removed. The equation to calculate the adsorbed amount of PET is as follows:

$$m_t = m_0 - m_w, \tag{2}$$

where m_t is the weight of PET adsorbed after t time, m_0 is the initial weight of PET in the solution, and m_w is the weight of unadsorbed PET. Based on a concentration of 300 mg/L, Zheng et al. [2] confirmed this as the saturation adsorption capacity of their aerogel sample , the initial weight of microplastic prepared for each PET solution was fixed at ~30.0 mg. The adsorption capacity results are presented in Figure 10.

After 18 hours, we recorded the adsorption capacity of 0.082 g of sc-PLA aerogel to be 54.01 mg g^{-1}, as studied, whose adsorption relied primarily on their porous structure [1,3]. Sc-PLA aerogel displayed greater adsorption capacity. Nonetheless, this result is inferior to aerogels enhanced with cationic modifications (i.e., chitosan, 2, 3-epoxypropyl trimethyl ammonium chloride, polyethyleneimine), which were reported to have adsorption capacities of MPs greater than 100 mg g^{-1} [1,2,3]. In contrast, sc-PLA lacks the advantage of chemisorption for optimal adsorption capacity. Yet, similar to untreated aerogels mentioned earlier, its adsorption can be directly linked to its porosity. Therefore, we furthered our explanation of this physisorption phenomenon by studying the adsorption kinetics of sc-PLA aerogel.

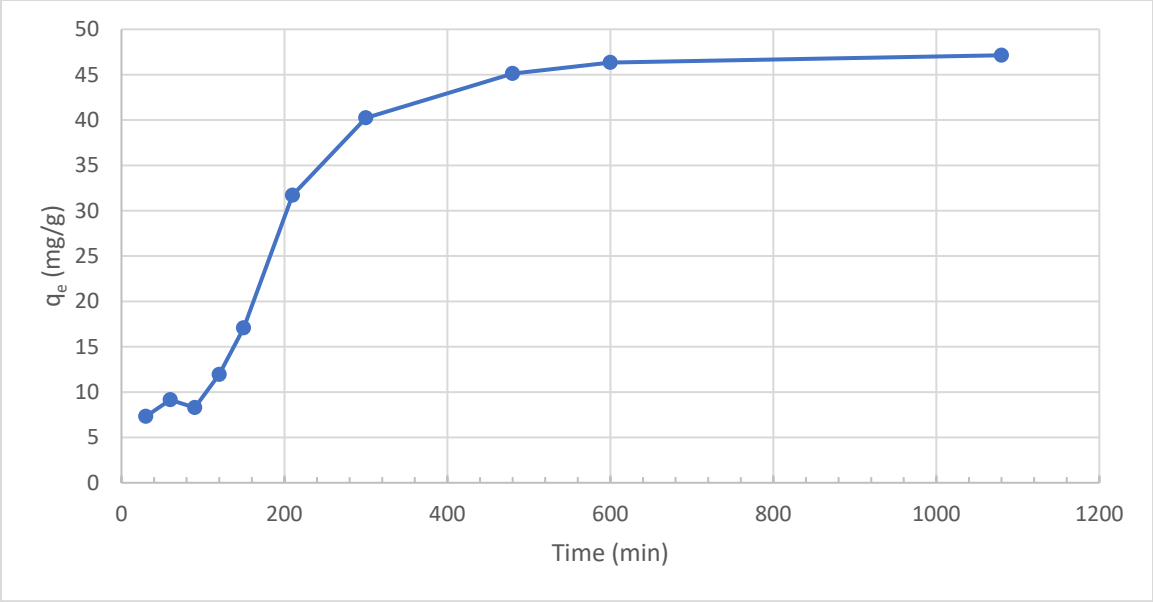


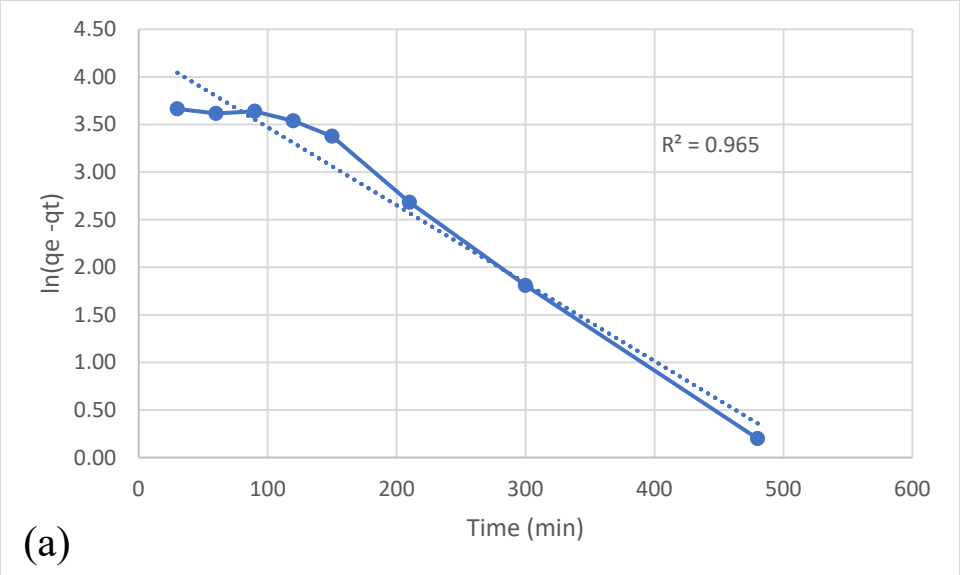
Figure 10. The adsorption capacity of experimental PET MPs in water being adsorbed by sc-PLA aerogel

Understanding the adsorption mechanism of PET MPs in water onto sc-PLA aerogel is crucial in determining the effectiveness of the selected material and the method of adsorbent manufacturing. Adsorption occurs via physisorption or chemisorption of MPs onto the surface of the adsorbent [2,19]. Two kinetic models commonly used for the empirical investigation of these adsorption mechanisms are pseudo-first-order and pseudo-second-order kinetics, which are respectively represented by the following equations [1,2,3]:

$$\ln(q_e - q_t) = lnq_e - k_1 t, \tag{3}$$

$$\frac{t}{q_t} = \frac{1}{k_2 q_e^2} + \frac{t}{q_e}, \tag{4}$$

where t is the adsorption time in min, q_e and q_t are the adsorption capacity at equilibrium and t, respectively. The rate constants for each of the kinetic models are represented by k_1 and k_2. Figure 11 displays the two kinetic models, including the coefficient determination value (R^2).



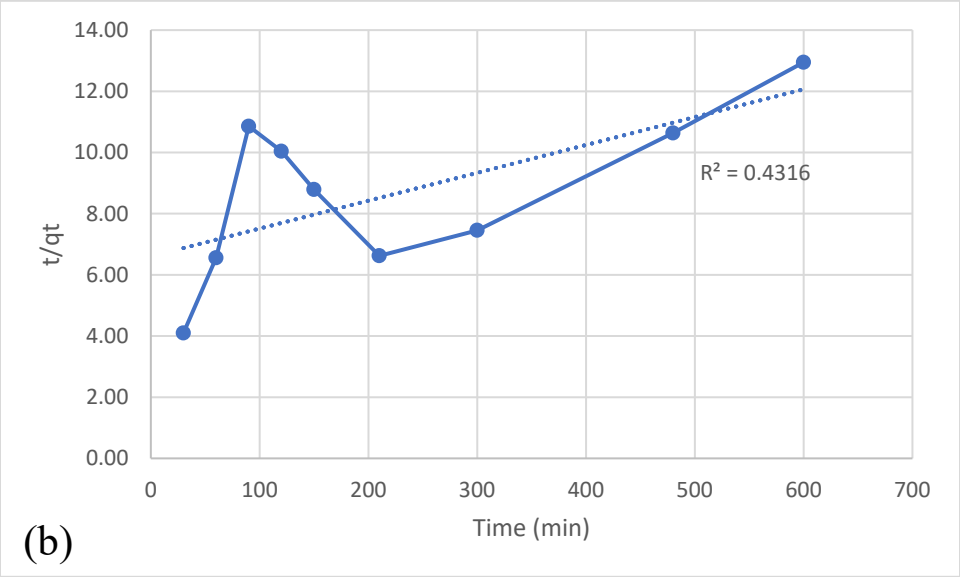


Figure 11. Adsorption (a) pseudo-first-order and (b) pseudo-second-order kinetic models of absorbed PET MPs in water onto sc-PLA aerogel at room temperature

The kinetic rates are 0.0082 and 0.00090 min^{-1} for the pseudo-first-order and pseudo-second-order models, respectively. The coefficient of determination (R^2) of the pseudo-first-order model (0.965) is significantly greater than that of the pseudo-second-order model (0.4316). The calculated q_e (46.47 mg g^{-1}) is also very close to the experimental result (46.34 mg g^{-1}). These results suggest that physisorption dominates the adsorption

mechanism of sc-PLA aerogel. More specifically, a weak van der Waals force (i.e., London disperse force) exists between the methyl groups on the surface of the PLA molecules and the carbonyl oxygen of the PET molecules.

Additionally, the poorly fitted pseudo-second-order model also confirms the lack of chemisorption in the optimization of the adsorption capacity of the sample. This is in contrast to the aerogel created by Zheng et al. [2], for instance, of which chemisorption proceeded via electrostatic interactions. The sample of Zhang et al. [1] even possessed greater rate of adsorption due to its abundance of active cationic sites. These kinetic parameters confirm the absence of strong chemical interactions and highlight the importance of the porous structure of sc-PLA aerogel in capturing MPs through physisorption.

Considering the impact of the porosity and the adsorption mechanism of the sc-PLA aerogel, we further investigated the different adsorption phases of PET MPs throughout the adsorbent via the intraparticle diffusion model (IDM). This kinetic model, also known as the Weber-Morris model, segments the adsorption to describe the rate-limiting step of the process [2]. The IDM graphs in Figure 11(a), (b), (c) were constructed according to parameters resulting from the following equation [2]:

$$q_t = k_{id} t^{0.5} + C \tag{5}$$

where k_{id} (mg g^{-1} t$^{0.5}$) represents the kinetic rate of a specific phase, and C is the intercept distance.

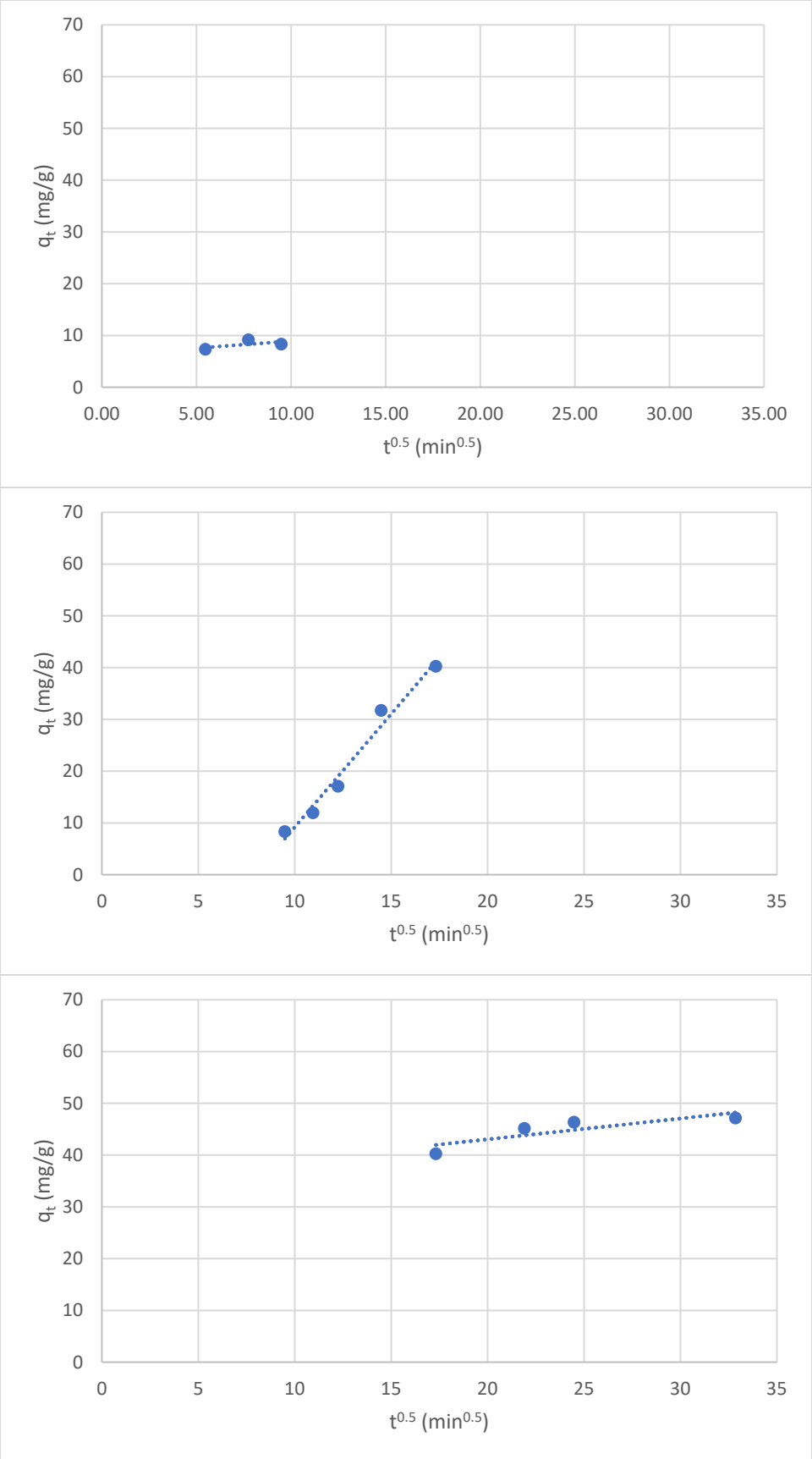

70
60
50
40
30
20
10
0
q_t (mg/g)
0.00
5.00
10.00
15.00
20.00
25.00
30.00
35.00
$t^{0.5}$ ($min^{0.5}$)
70
60
50
40
30
20
10
0
q_t (mg/g)
0
5
10
15
20
25
30
35
$t^{0.5}$ ($min^{0.5}$)
70
60
50
40
30
20
10
0
q_t (mg/g)
0
5
10
15
20
25
30
35
$t^{0.5}$ ($min^{0.5}$)

Figure 12. Intraparticle diffusion models in three adsorption phases, external film diffusion (a), interparticle diffusion (b), and saturation (c), of PET MPs adsorbed by sc-PLA aerogel at 25°C

An IDM provides additional information about the adsorption of the adsorbate within the structure of the adsorbent. It is specifically useful for porous, dimensionally thick adsorbents such as sc-PLA aerogel [2]. A typical model divides the adsorption process into three phases, namely, external film diffusion, intraparticle diffusion, and saturation [2,23,24]. Presented in Figure 12(a), (b), (c), the data were fitted into three separated linear models representing three different adsorption phases. The external film diffusion phase dominated the first ~90 minutes, during which PET MPs were transported from the bulk solution to the external surface of the aerogel. In the subsequent ~3.5 hours, the adsorption rate increased markedly during the intraparticle diffusion phase, as the adsorbate crossed the boundary layer and began diffusing into the internal porous matrix of the aerogel. Finally, after ~8 hours, the adsorption process approached equilibrium, indicating the onset of the saturation phase, where the available adsorption sites became limited. Table 2 presents all the IDM parameters of three adsorption phases.

Table 2. Parameters of intraparticle diffusion model for sc-PLA aerogel, representing three phases: external film diffusion (1), interparticle diffusion (2), and saturation (3)

k_{id1} (mg/g m^{-1})	k_{id2} (mg/g m^{-1})	k_{id3} (mg/g m^{-1})	R_1^2	R_2^2	R_3^2	C_1	C_2	C_3
0.2699	4.368	0.4021	0.3513	0.9773	0.7190	6.210	-34.49	35.00

The interparticle diffusion phase has the most significant impact on the adsorption process due to its kinetic rate [2] and the best linear fit (i.e., highest R^2 value) [23,24]. Noticeably, the lower adsorption rate observed during the external film diffusion phase contrasts with findings from other studies on modified adsorbents [2,23,24], where this step predominantly influenced the entire process. This discrepancy may be attributed to weak van der Waals forces between the PET MPs and the sc-PLA aerogel, suggesting that surface adsorption did not contribute significantly. Nonetheless, the non-zero C values (i.e., y-intercept) indicate that the overall process is complex and governed by multiple mechanisms, implying that while interparticle diffusion plays a major rolre, it is not the only rate-limiting step [2,23].

CHAPTER 4

CONCLUSION

An sc-PLA aerogel was manufactured via a facile procedure that required no complex modifications, with the objective of removing PET MPs from water. The prominent presence of stereocomplex crystals, confirmed via XRD analysis, enhanced the aerogel's mechanical properties and, more importantly, its porosity. Analysis of SEM images confirmed the porous adsorption sites dominated by macropores of >100 μm , appropriate for the adsorption and capturing of the targeted micron-sized PET. Adsorption isotherm with nitrogen gas revealed the presence of micropores and mesopores in optimizing the overall surface area. The adsorption of sc-PLA aerogel proceeded primarily via physisorption, lacking the optimized interactions provided by chemisorption mechanisms typical of other cationic modified aerogels in literature. Specifically, the aerogel's porous structure was responsible for capturing othe majority of MPs during the adsorption experiment, while the role of surface adsorption was minimal. Nonetheless, this study further supports the potential of sc-PLA aerogel as a safe, non-toxic, and biodegradable material for MPs removal via adsorption. Future research should consider improving the adsorption capacity of the aerogel via chemical modifications, porosity design, or other tunable manufacturing parameters.

REFERENCES

1. Zhuang, J.; Rong, N.; Wang, X.; Chen, C.; Xu, Z. Adsorption of small size microplastics based on cellulose nanofiber aerogel modified by quaternary ammonium salt in water. *Separation and Purification Technology* **2022***, 293*, 121133.

2. Zheng, B.; Li, B.; Wan, H.; Lin, X.; Cai, Y. Coral-inspired environmental durability aerogels for micron-size plastic particles removal in the aquatic environment. *J. Hazard. Mater.* **2022***, 431*, 128611.

3. Zhuang, J.; Pan, M.; Zhang, Y.; Liu, F.; Xu, Z. Rapid adsorption of directional cellulose nanofibers/3-glycidoxypropyltrimethoxysilane/polyethyleneimine aerogels on microplastics in water. *Int. 8. Biol. Macromol.* **2023***, 235*, 123884.

4. Chen, P.; Bai, D.; Tang, H.; Liu, H.; Wang, J.; Gao, G.; Li, L. Polylactide aerogel with excellent comprehensive performances imparted by stereocomplex crystallization for efficient oil-water separation. *Polymer* **2022***, 255*, 125128.

5. Deng, Y.; Zhang, N.; Huang, T.; Lei, Y.; Wang, Y. Constructing tubular/porous structures toward highly efficient oil/water separation in electrospun stereocomplex polylactide fibers via coaxial electrospinning technology. *Appl. Surf. Sci.* **2022***, 573*, 151619.

6. Milovanovic, S.; Markovic, D.; Pantic, M.; Pavlovic, S. M.; Knapczyk-Korczak, J.; Stachewicz, U.; Novak, Z. Development of advanced floating poly(lactic acid)-based materials for colored wastewater treatment. *Journal of Supercritical Fluids* **2021***, 177*.
7. Benito-González, I.; López-Rubio, A.; Gómez-Mascaraque, L. G.; Martínez-Sanz, M. PLA coating improves the performance of renewable adsorbent pads based on cellulosic aerogels from aquatic waste biomass. *Chem. Eng. J.* **2020***, 390*, 124607.

8. Krishnan, V. G.; Praveena, N. M.; Raj, R. B. A.; Mohan, K.; Gowd, E. B. Thermoreversible Gels of Poly(l-lactide)/Poly(d-lactide) Blends: A Facile Route to Prepare Blend α-Form and Stereocomplex Aerogels. *ACS Applied Polymer Materials* **2023***, 5*, 1556 – 1564.

9. Qi, L.; Zhu, Q.; Cao, D.; Liu, T.; Zhu, K.; Chang, K.; Gao, Q. Preparation and Properties of Stereocomplex of Poly(lactic acid) and Its Amphiphilic Copolymers Containing Glucose Groups. *Polymer* **2020**, *12*(4), 760.

10. Cui, W.; Wei, X.; Luo, J.; Xu, B.; Zhou, H.; Wang, X. CO2-assisted fabrication of PLA foams with exceptional compressive property and heat resistance via introducing well-dispersed stereocomplex crystallites. *Journal of CO2 Utilization* **2022***, 64*, 102184.

11. Jia, L. J.; Phule, A. D.; Yu, Z.; Zhang, X.; Zhang, Z. X. Ultra-light poly(lactic acid)/SiO2 aerogel composite foam: A fully biodegradable and full life-cycle sustainable insulation material. *Int. J. Biol. Macromol.* **2021***, 192*, 1029-1039.

12. Trofimchuk, E. S.; Potseleev, V. V.; Khavpachev, M. A.; Moskvina, M. A.; Nikonorova, N. I. Polylactide-Based Porous Materials: Synthesis, Hydrolytic Degradation Features, and Application Areas. *Polymer Science - Series C* **2021***, 63*, 199 – 218.

13. Xie, Y.; Lan, X.; Bao, R.; Lei, Y.; Cao, Z.; Yang, M.; Yang, W.; Wang, Y. High-performance porous polylactide stereocomplex crystallite scaffolds prepared by solution blending and salt leaching. *Materials Science and Engineering: C* **2018***, 90*, 602-609.

14. Alhaj, M.; Narayan, R. Scalable Continuous Manufacturing Process of Stereocomplex PLA by Twin-Screw Extrusion. *Polymers* **2023**, *15*(4), 922.

15. Yin, G-Z.; Yang, X-M.; López A.; Ao, X.; Wang, M-T.; Molleja, J.; Wang, D-Y. PLA aerogel as a universal support for the typical organic phase change energy storage materials. *Journal of Energy Storage* **2023**, *73*, 108869.

16. Salerno, A.; Domingo, C. Making microporous nanometre-scale fibrous PLA aerogels with clean and reliable supercritical CO_2 based approaches. *Microporous and Mesoporous Materials* **2014**, *184*, 162-168.

17. Adams, F. In *X-RAY ABSORPTION AND DIFFRACTION | Overview;* Worsfold, P., Townshend, A. and Poole, C., Eds.; Encyclopedia of Analytical Science (Second Edition); Elsevier: Oxford, 2005; pp 365–377.

18. Akhtar, K., Khan, S.A., Khan, S.B., Asiri, A.M. Scanning Electron Microscopy: Principle and Applications in Nanomaterials Characterization. *Sharma, S. (eds) Handbook of Materials Characterization*. Springer: Cham, 2018; pp 113-145.

19. Juhász, L.; Modován, K.; Gurikov, P.; Liebner, F.; Fábián, I.; Kalmár, J.; Cserháti, C. False Morphology of Aerogels Caused by Gold Coating for SEM Imaging. *Polymers* **2021**, *13*(4), 588.

20. Durkee, J. B. In *Chapter 4 - "Tailpipe" Treatment of Fugitive Solvent Emissions;* Durkee, J. B., Ed.; Cleaning with Solvents: Methods and Machinery; William Andrew Publishing: Oxford, 2014; pp 177–234.

21. Miao, X.; Sun, D. Graded/Gradient Porous Biomaterials. *Materials* **2010**, *3*(1), 26-47.

22. Kanetake, N.; Kobashi, M. Innovative processing of porous and cellular materials by chemical reaction. *Scripta Materialia* **2006**, *54*, 521-525.

23. Sun. C.; Wang, Z.; Chen, L.; Li, F. Fabrication of robust and compressive chitin and graphene oxide sponges for removal of microplastics with different functional groups. *Chemical Engineering Journal* **2020**, *393*, 124796.

24. Wang, J.; Guo, X. Rethinking of the intraparticle diffusion adsorption kinetics model: Interpretation, solving methods and applications. *Chemosphere* **2022**, *309*(2), 136732.